Affine Arithmetic For Efficient And Reliable Resolution of Weather-Based Uncertainties in Optimal Power Flow Problems

Affine Arithmetic For Efficient And Reliable Resolution of Weather-Based Uncertainties in Optimal Power Flow Problems

Guido Coletta[a,*], Alfredo Vaccaro[a], Domenico Villacci[a], Duo Fang[b], Sasa Z. Djokic[b]

[a] *Engineering Department, DING, University of Sannio, Piazza Roma, 21, Benevento, 82100, Italy*
[b] *School of Engineering, The University of Edinburgh, Faraday Building, 4.112, Edinburgh EH9 3JL, Scotland, UK*

Abstract

The massive diffusion of renewable power generators in existing power grids introduces large uncertainties in power system operation, hindering their hosting capacity, and introducing several critical issues in network management. To address these challenging issues, weather-based optimal power flow has been recognized as one of the most promising enabling methodology for increasing the system flexibility by exploiting the real power components loadability. Anyway, the deployment of this technique in a real operation scenario could be seriously compromised due to the effects of data uncertainty, which could sensibly affect both the generated/demanded power profiles, and the components thermal modeling. In this context, the research for reliable techniques aimed at representing and managing these uncertainties represents one of the most relevant problem to solve. Armed with such a vision, this paper advocates the role of Affine Arithmetic in reliable solving weather-based OPF problems in the presence of multiple and correlated uncertainties. Experimental results obtained on a real case study, which is based on a congested portion of a transmission system characterized by a massive pervasion of wind generators, will be presented and discussed in order to assess the benefits deriving by the application of the proposed method.

Keywords: Uncertainty Management, Self-Validated Computing, Optimal Power Flow, Dynamic Thermal Rating, Electro-Thermal OPF

Nomenclature

f_{obj}	Objective function	$[-]$
$\boldsymbol{x}$	Set of the control variables	$[-]$
$\boldsymbol{P}_{gen}$	Set of the generated active powers at PV buses	$[MVA]$
$\boldsymbol{Q}_{gen}$	Set of the generated reactive powers at PV buses	$[MVAr]$
$\boldsymbol{V}_m$	Set of the voltage magnitudes at PV buses	$[V]$
$\boldsymbol{V}_a$	Set of the voltage angle at PV buses	$[rad]$
$\boldsymbol{P}^i_{gen}$	Set of the i^{th} partial deviations of the generated active powers at PV buses	$[MVA]$
$\boldsymbol{Q}^i_{gen}$	Set of the i^{th} partial deviations of the generated reactive powers at PV buses	$[MVAr]$
$\boldsymbol{V}^i_m$	Set of the i^{th} partial deviations of the voltage magnitudes at PV buses	$[V]$
$\boldsymbol{V}^i_a$	Set of the i^{th} partial deviations of the voltage angle at PV buses	$[rad]$
$P_{cut,i}$	Curtailed power at i^{th} wind generators	$[MVA]$
$\boldsymbol{V}^{Re}$	Set of voltage real parts	$[V]$
$\boldsymbol{V}^{Im}$	Set of voltage imaginary parts	$[V]$

*Corresponding author
Email addresses: gcoletta@unisannio.it (Guido Coletta), vaccaro@unisannio.it (Alfredo Vaccaro), villacci@unisannio.it (Domenico Villacci), D.Fang@ed.ac.uk (Duo Fang), sasa.djokic@ed.ac.uk (Sasa Z. Djokic)

PV	Set of buses where active power and voltage magnitudes are fixed	$[-]$
$P\theta$	Set of buses where active power and voltage angle are fixed	$[-]$
PQ	Set of buses where active and reactive power are fixed	$[-]$
N	Buses number	$[-]$
V_i^{min}	Minimum voltage magnitude at i^{th} bus	$[V]$
V_i^{max}	Maximum voltage magnitude at i^{th} bus	$[V]$
V_i	Voltage magnitude at i^{th} bus	$[V]$
$P_{gen,i}^{min}$	Minimum generated active power at i^{th} bus	$[MVA]$
$P_{gen,i}^{max}$	Maximum generated active power at i^{th} bus	$[MVA]$
$P_{gen,i}$	Generated active power at i^{th} bus	$[MVA]$
$Q_{gen,i}^{min}$	Minimum generated reactive power at i^{th} bus	$[MVAr]$
$Q_{gen,i}^{max}$	Maximum generated reactive power at i^{th} bus	$[MVAr]$
$Q_{gen,i}$	Generated reactive power at i^{th} bus	$[MVAr]$
$P_{inj,i}^{fix}$	Fixed injected active power at i^{th} bus	$[MVA]$
$Q_{inj,i}^{fix}$	Fixed injected reactive power at i^{th} bus	$[MVAr]$
y_{ij}	Magnitude of the i,j element of nodal admittance matrix	$[\Omega^{-1}]$
$\theta_i j$	Angle of the i,j element of nodal admittance matrix	$[rad]$
δ_i	Angle voltage at i^{th} bus	$[rad]$
I_k	Current magnitude at the k^{th} connecting line	$[A]$
I_k^{max}	Maximum current magnitude at the k^{th} connecting line	$[A]$
N_l	Number of lines	$[-]$
T_k	Conductor temperature of k^{th} line	$[\,^{\circ}\mathrm{C}]$
$G_{i,j}$	Real part of the i,j element of nodal admittance matrix	$[\Omega^{-1}]$
$B_{i,j}$	Imaginary part of the i,j element of nodal admittance matrix	$[\Omega^{-1}]$
v_w^{for}	Forecasted wind speed	$[m \cdot s^{-1}]$
$\hat{v}_w$	Affine wind speed	$[m \cdot s^{-1}]$
$\hat{P}_{g,i}$	Affine active power generated by the i^{th} bus	$[MVA]$
$\hat{P}_{d,i}$	Affine active power absorbed by the i^{th} bus	$[MVA]$
$\hat{Q}_{d,i}$	Affine reactive power absorbed by the i^{th} bus	$[MVAr]$
$P_{d,i}^{nom}$	Nominal active power absorbed by the i^{th} bus	$[MVA]$
$Q_{d,i}^{nom}$	Nominal reactive power absorbed by the i^{th} bus	$[MVAr]$

1. Introduction

In recent years there have been radical changes in planning and operating power systems, which were mainly induced by the need of reducing the pollutant emissions and the primary energy consumption, supporting the sustainable development of the energy sector. In this context, the main international treaties, such as the Kyoto Protocol and the European 2020 climate & energy package, stimulated the large scale diffusion of Renewable Power Generators (RPGs) all over the transmission and distribution networks, supporting the transition from a centralized to a distributed generation paradigm. Even though these technologies lead to sensible economical and environmental advantages, their large scale diffusion in existing power grids causes many critical issues that need to be properly addressed [1].

In particular, due to the wind and photo-voltaic generation unpredictability the system operators have to schedule more reserve resources aimed at instantaneously balancing the generated power with the loads and the system losses. Furthermore, the electricity market rules, which were designed to stimulate the diffusion of renewable technologies, induce the traditional generators to work far from their optimal operation conditions, increasing their marginal costs and emissions, hence reducing the environmental benefits of RPGs.

The large scale penetration of RPGs in distribution networks implies another serious drwaback, which derives from the lose of confidence in one of the principal assumption in distribution system planning and operation, namely, the unidirectional power flows among decreasing voltage level direction. In this context, the power flows redistribution casued by RPGs leads the system components to operate closest to

their thermal limits, increasing the risk of network congestion [2]. To manage the contingencies induced by RPGs, the System Operators (SOs) have to implement proper corrective actions, i.e. market splitting and renewable power curtailments, which have severe economic consequences, since they modify the "natural" market equilibrium. To reduce the economic impacts of network contingencies, SOs are willing to strengthen the critical interconnections by increasing the network meshing through the construction of new lines and primary stations [3]. Anyway, the development of this long-term strategy is hindered by several limitations, mainly due to the difficulties in updating and constructing new electrical infrastructures.

Consequently, the conceptualization of advanced tools aimed at reliably improving the power components exploitation represents one of the most promising enabling methodology for supporting a massive integration of RPGs, increasing the power system flexibility, and reducing the risk of contingency [4]. Traditionally, SOs compute the power component thermal limits by considering the worst case conditions for the heat exchange process, such as maximum solar irradiation, minimum convection cooling rate. But, these conditions insist on the conductors only for a small percentage of their lifetime, while in the other conditions the infrastructure is sensibly underemployed. To reliably improve the components exploitation, a very promising technique is the Dynamic Thermal Rating (DTR) assessment, which aims at dynamically evaluating the thermal rating of the congested infrastructure on the basis of the actual weather conditions insisting on the conductor.

The benefits deriving by the application of DTR techniques in existing power systems have been assessed in several papers, which proposed different solution methodologies, including those based on first order components thermal models, or integrating distributed sensors for the direct measurement of the conductor temperature [5]. These techniques, if integrated in advanced optimization frameworks, known as Weather Condition-based Optimal Power Flow (W-OPF) or Electro-Thermal OPF (ET-OPF), could reliably improve the components loadability, enhancing the congestion management flexibility, and maximizing the RPGs' exploitation [6,7,8]. The implementation of these frameworks could in principle allow the system operator to exploit the advantages of the DTR procedures, taking into account both the electrical and thermal state variables, and to extract actionable intelligence from the large and heterogenoeus data streaming generated by pervasive monitoring systems installed on the power systems [3]. Despite these benefits, the application of W-OPF analyses in real operation scenario is still at its infancy, and several open problems need to be addressed in order to enhance their robustness.

In particular, some criticalities raised in several papers concern with the reliable assessment of the hot-spot temperature of overhead lines, since, especially in area with complex orographic characteristics, the identification of the critical span along the line route is a very complex spatial-temporal problem. Several approaches have been proposed to solve this complex issue, including the adoption of distributed sensor networks [9], and numerical weather prediction models [10].

Another serious limitations of W-OPF approaches is that they are based on deterministic computing paradigms, which do not consider the effects of the data uncertainties affecting the input variables of the optimization problem. In particular, non-programmable energy sources unpredictability increase the uncertainty of the injected power profiles, affecting the power flows on the entire power system. Furthermore, the variables ruling the component thermal dynamics are always affected by strong uncertainties, which are mainly induced by the spatial profiles of the meteorological variables, and the variation of the components thermal parameters. All these uncertainties could sensibly affect the robustness of the computed solutions, compromising the effectiveness of the corresponding loading strategies [11,12].

To face this issue, several class of methods can be adopted, including those based on the probability theory [13,14,15], approximation techniques [16,17,18,19,20,21,22] and sample based methodologies. Experimental results obtained on several case studies demonstrated that the performances of these solution algorithms mainly depend on the consistency and the statistical proprieties of the input data, which, unfortunately, can be rarely assumed in solving W-OPF problems in a real operating scenario.

In order to overcome these limitations, the deployment of self-validated computing frameworks represents a promising research direction. The simpler of these approaches is Interval Arithmetic, which is not particularly useful in solving W-OPF problems, since it tends to produce results whose ranges are too much higher than the real ones because of the error explosion phenomena [23]. To solve this problem a more complex range analysis technique based on Affine Arithmetic (AA), which keeps track of the uncertainties dependencies and propagation by assigning an "error symbol" to each uncertainty source, could be adopted [24]. AA has

been successfully applied to solve complex optimization problems in the presence of multiple and correlated uncertainties[25], allowing to reliably satisfy both equality and inequality constraints. Hence, it could play an important role in solving uncertain W-OPF problems, by reliably managing the large data uncertainty affecting both the DTR computing process, and the generated/demanded power profiles.

Furthermore, a plausible mid-term future scenario might introduce additional uncertainty ranges in power system operation due to the introduction of new technologies (e.g. distributed energy storage systems and electric vehicles operating in Vehicle to Grid, V2G, configuration, characterized by shifting from power consumption (loads) to power production (generators and energy storage), which could then absorb or inject power into the grid depending on their particular operating state. The presented AA-based methodology can effectively handle these additional uncertainties by an affine form whose bounds are the maximum and minimum generated or demanded power, ranging from the maximum consumed load power (negative value) up to the maximum produced power injected into the grid (positive).

In this context, it is important also to underline that the electricity market dynamics could sensibly affect the number, the magnitude and the location of power transactions. To represent these complex phenomena, it is possible to consider the energy prices uncertainty (and, in particular, the uncertainty affecting the local marginal prices). These uncertainties will affect the wind curtailment strategies, as well as the power profiles injected by conventional controllable generators. However, due to the lack of actual data characterizing the market dynamics for the considered network area, this has not been addressed in the presented case study.

Armed with such a vision, this paper proposes an AA-based computing framework, which aims at solving uncertain W-OPF analysis, by explicitly considering the effects of the components' thermal dynamics on the system constraints. The main benefits deriving by the application of this approach are:

- There is a strict and complex correlation between the components' thermal constraints and wind power production. For example, within the operational region of wind turbine (i.e., between the cut-in and cut-out wind speeds), if wind speed increases, wind power production does the same, but also the loading capability of the power components increases, allowing to dispatch more energy produced by renewable sources. This concept can be effectively represented in the AA-based computing framework by defining a shared error symbol between the wind speed, wind power production and components' loading capability.

- both system constraints and OPF solutions are computed according to the same AA-based paradigm, which allows describing the effects of uncertainty propagation from observable and measurable data (i.e. wind speed) to system constraints (conductor temperature) and problem solutions.

- the application of AA-based computing allows a robust solution of the optimization problem, considering all the possible instances of the exogenous uncertainties.

To demonstrate these benefits, measurements and field data obtained from a real case study, which is based on a portion of a heavily congested transmission system characterized by a large penetration level of wind generators, will be presented and discussed. The operation of this actual power network is a challenging issue to address, since the nominal power of the wind generators installed in the considered area is almost 10 times greater than the corresponding peak load demand and the power lines connecting the wind generators with the national power system are operating very close to their thermal limits. Hence, in the presence of high wind speed patterns, the power network could be affected by multiple congestions and proper power curtailment strategies should be implemented in order to maximize line utilization and mitigate negative effects of congestions.

The rest of the paper is organized as follows: in Section 2 mathematical frameworks of DTR and W-OPF has been presented in detail. Then, Section 3 provides mathematical of Affine Arithmetic and AA-based OPF and W-OPF problems, giving instruments to solve them through the traditional algorithms of Optimizaion theory. Eventually, Section 4 will present results of the application the proposed methodology on a real case study.

2. Problem Formulation

2.1. Dynamic Thermal Rating

The Dynamic Thermal Rating is a loading strategy, which aims at exploiting the real capability of electric power components by dynamically computing their thermal ratings, on the basis of the real meteorological conditions insisting on the components.

The assessment of the hot-spot temperature is a necessary prerequisite for the correct application of the DTR paradigm. The methods currently adopted to face this issue can be classified as [5]:

- Indirect Methods or Weather-Based Methods
- Direct Methods

The first ones allow estimating the conductor temperature by solving a first order thermal model, taking as inputs its real loading and the worst-case weather conditions insisting on the component [26]. The main benefits deriving by the application of these methods mainly derive from their low technological requirements, which make straightforward their deployment in existing optimization frameworks. On the other hand, the component thermal estimations computed by these techniques could be affected by large data uncertainties, which mainly depends on the integrity of the model input data.

Direct methods allow overcoming this limitation, by directly measuring the spatial profile of the conductor temperature (i.e. by fiber optical-based distributed sensing systems), or by deploying a set of sensors in the most probable critical spans in order to infer the hot-spot temperature [27,28]. Although these methods allow improving the thermal estimation reliability, they require complex sensors aimed at continuously measuring the conductor temperature and/or the weather variables at conductor height, which is a challenging issue to address.

Recently, thanks to the large-scale deployment of Phasor Measurement Units (PMUs), new computing paradigms based on time-synchronized signal processing for DTR have been proposed in the literature [5,3]. These approaches aim at processing the time-synchronized phasors acquired by PMUs for estimating the electrical component parameters, and empirically inferring the corresponding component temperature [29]. Although the application of this DTR paradigm exhibits several advantages over the aforementioned direct and indirect approaches, since it does not require the need for deploying a dedicated and distributed sensing architecture, it allows estimating the average conductor temperature, which could be sensible different from the hot-spot.

On the basis of these argumentation, this study relies on Weather-Based Methods based on the thermal model proposed in *"IEEE Standard 738-2012 for Calculating the Current-Temperature Relationship of Bare Overhead Conductors"* [26], which is one of the most used approach for DTR in W-OPF analyses.

This thermal modeling methodology is based on the integration of the following first order thermal model:

$$\frac{d}{dt}(T_{avg}) = \frac{1}{mC_p}\left[q_s + I^2R(T_{avg}) - q_c - q_r\right] \tag{1}$$

where:

q_s	Solar heat gain rate per unit length
$I^2R(T_{avg})$	Joule-Effect heat gain
q_c	Convection heat loss rate per unit length
q_r	Radiated heat loss rate per unit length

Further details on the computation of these terms can be found in [26].

2.2. Weather Condition based-OPF

The main idea of W-OPF analysis is to integrate a DTR technqiue in a conventional OPF formulation, by replacing the static component limits based on maximum ampacity constraints, with dynamic component limits based on the maximum hot-spot temperature. The latter can be estimated according to the

weather-based DTR, by solving a first order differential equation relating the hot-spot temperature with the environmental variables measured on the critical span, and the worst case estimation of the conductor thermal parameters. The overall optimization problem in a certain time interval can be formalized as follows.

$$
\begin{aligned}
\min_{\mathbf{x}} \quad & f_{obj}(\mathbf{x}) \\
\text{s.t.} \quad & V_i^{min} \leq V_i \leq V_i^{max} && \forall i \in [1,\dots,N] \\
& P_{gen,i}^{min} \leq P_{gen,i} \leq P_{gen,i}^{max} && \forall i \in \{PV;V\theta\} \\
& Q_{gen,i}^{min} \leq Q_{gen,i} \leq Q_{gen,i}^{max} && \forall i \in \{PV;V\theta\} \\
& T_k < T_k^{max} && \forall k \in [1,\dots,N_l] \\
& P_{inj,i}^{fix} = V_i \sum_{j=1}^{N} V_j \, y_{ij} \, \cos(\theta_{ij} + \delta_j - \delta_i) && \forall i \in [1,\dots,N] \\
& Q_{inj,i}^{fix} = V_i \sum_{j=1}^{N} V_j \, y_{ij} \, \sin(\theta_{ij} + \delta_j - \delta_i) && \forall i \in [1,\dots,N] \\
& T_k = T_s + \frac{1}{mC_p} \int_{t_s}^{t_f} \big(q_s + I_k^2 \, R(T_k) - q_c - q_r\big) d\tau && \forall \, k \in [1,\dots,N_l]
\end{aligned}
\tag{2}
$$

where the state variables are described by the following vector:

$$
\mathbf{x} = [\mathbf{P}_{gen}, \mathbf{Q}_{gen}, \mathbf{V}_m, \mathbf{V}_a] \tag{3}
$$

2.3. Uncertainty Sources in W-OPF

The solution of W-OPF problem formalized in (2) requires the knowledge of input data, which can be affected by large uncertainties, mainly deriving by measurement, estimation or forecasting errors.

In particular, the component parameters and the input variables of the thermal model (1) are affected by large uncertainties, which can be classified as:

- forecasting/measurement uncertainty
- lack of knowledge/approximation

Quantities like line current, environmental temperature, wind speed and direction, sun irradiation are affected by large uncertainty induced by measurement or forecasting errors, which characterize real-time operation and pre-dispatch, respectively.

Moreover, since hygrometric air proprieties is measured or computed as function of the environmental temperature through polynomial regression, they introduce further uncertainty in the thermal model. Furthermore, electric resistance temperature coefficient, absorption and emission heat exchange factors represent a further origin of error, since their actual values changes with the conductor ageing and degradation state.

Further uncertainties affecting W-OPF analyses derive by the randomness characterizing the power profiles generated by non-programmable RPGs, which are influenced by the unpredictability of the renewable energy sources, and the intrinsic complexity of the electricity market price dynamics, which influence the number of power transactions that are carried over the system.

Under such conditions, reliable solution methods that incorporate the effects of data uncertainty into the W-OPF analysis are required. These algorithms would allow system operators to address both uncertainty representation and uncertainty propagation, thus allowing them to evaluate the level of confidence of W-OPF studies.

3. Solving uncertain W-OPF problems by Affine Arithmetic

3.1. Element of Affine Arithmetic

Affine Arithmetic (AA) is a Self Validated Computing framework that intrinsically keeps track of data uncertainty propagation, mitigating the error explosion problem characterizing traditional Interval Analysis. The main feature of AA is the introduction of statistically correlated error symbols that, in some way, take into account the statistical dependence of two variables affected by the same uncertainty source [30]. Hence, in the AA-domain each uncertain elementary quantity, x, can be expressed as an affine form , $\hat{x}$, which has the following form:

$$\hat{x} = x_0 + x_1\epsilon_1 + x_2\epsilon_2 + \cdots + x_n\epsilon_n \tag{4}$$

where x_0, $[x_1 \dots x_n]$ and $[\epsilon_1 \dots \epsilon_n] \in [0, 1]$ are the central value, the partial deviations and the noise symbols of the affine form, respectively.

The coefficients x_i are finite floating-point numbers, and the ϵ_i are symbolic real variables (noise) whose values are unknown, but assumed to lie in the interval $U = [-1;\ 1]$. Each noise symbol represents an independent component of the total uncertainty of the ideal quantity, x; the corresponding coefficient gives the magnitude of that component.

The fundamental invariant of affine arithmetic states that, for every AA operation, there is a single assignment of values from U to each of the noise variables in use that makes the value of every affine form $\hat{x}$ equal to the true value of the corresponding ideal quantity, x.

The key feature of AA is that the same noise symbol may contribute to the uncertainty of two or more quantities arising in the evaluation of an expression, when the sharing of the noise symbols indicates (partial) dependency between the underlying quantities $\hat{x}$ and $\hat{y}$, determined by the corresponding coefficients x_i and y_i.

Correlation between uncertain variables is considered by sharing error symbol between two different affine quantities. Hence, two variable sharing error symbols are affected by the same uncertainty seeds and are correlated someway.

Dependent uncertainty sources are modeled by sharing error symbols between variables. For example:

- Case 1: Independent uncertainty sources:

$$\hat{x}_1 = 1 + 2\epsilon_1 + 0\epsilon_2 = [-1\ 1] \tag{5}$$
$$\hat{x}_2 = 1 + 0\epsilon_1 + 2\epsilon_2 = [-1\ 1] \tag{6}$$
$$\hat{x}_1 - \hat{x}_2 = 0 + 2\epsilon_1 - 2\epsilon_2 = [-4\ 4] \tag{7}$$

- Case 2: Dependent uncertainty sources:

$$\hat{x}_1 = 1 + 2\epsilon_1 = [-1\ 1] \tag{8}$$
$$\hat{x}_2 = 1 + 2\epsilon_1 = [-1\ 1] \tag{9}$$
$$\hat{x}_1 - \hat{x}_2 = 0 + 0\epsilon_1 = \emptyset \tag{10}$$

Each affine form, $\hat{x}$, can be managed as an interval by defining the equivalent overall deviation $r = \sum_{i=1}^{n} |x_i|$, representing the minimum radius that contains all the allowable value of $\hat{x}$, whichever is the combination of the independent component of the noise symbols set, ϵ. The correspondent interval can be expressed as:

$$\bar{x} = [x_0 - r,\ x_0 + r]$$

Let us define some useful operators in the AA domain.

Definition 1 (mid)**.** *The "mid" operator returns the central value of an affine form $\hat{x}$.*

$$\text{mid}(\hat{x}) = x_0 \tag{11}$$

Definition 2 (rad)**.** *The "rad" operator returns the radius of an affine form* $\hat{x}$*.*

$$\mathrm{rad}(\hat{x}) = \sum_{i}^{N_{err}} |x_i| \tag{12}$$

Definition 3 (inf)**.** *The "inf" operator returns the lower bound of an affine form* $\hat{x}$*.*

$$\inf(\hat{x}) = x_0 - \mathrm{rad}(\hat{x}) \tag{13}$$

Definition 4 (sup)**.** *The "sup" operator returns the upper bound of an affine form* $\hat{x}$*.*

$$\sup(\hat{x}) = x_0 + \mathrm{rad}(\hat{x}) \tag{14}$$

Moreover, it is possible to define proper mathematical operators for AA-based computing. In particular, to compute a general function of two affine forms $\hat{x}$ and $\hat{y}$, it is necessary to find an application $\hat{F}$ such that $\hat{z} = \hat{F}(\hat{x}, \hat{y})$ is coherent with respect to the correspondent ideal quantity $z = f(x, y)$. If the function f is linear, then its affine extensions is trivial, since it can be expressed through a linear combination of the partial deviations of the "primitive" noise symbols, as follows:

$$\alpha\hat{x} + \beta\hat{y} + \gamma = (\alpha x_0 + \beta y_0 + \gamma) + +\epsilon_1(\alpha x_1 + \beta y_1) + \cdots + \epsilon_n(\alpha x_n + \beta y_n) \tag{15}$$

On the other hand, if f is non-linear, then it should be approximated by a first order polynomial that well fit the function in a specified range, and a new noise symbol representing the corresponding approximation error should be considered:

$$\hat{f}^{app} = z_0 + \epsilon_1 z_1 + \epsilon_2 z_2 + \cdots + \epsilon_n z_n + \epsilon_k z_k$$

where the new noise symbol $\epsilon_k x_k$ and the corresponding partial deviation represent the endogenous uncertainty.

Hence, a non-affine operation between two affine forms $\hat{x}$ and $\hat{y}$ can be recasted as $\alpha\hat{x} + \beta\hat{y} + \gamma$, where coefficients α, β and γ need to be identified. To this aim, two possible approaches can be adopted, namely the Chebyshev approximation and the minimum range[31,32].

3.1.1. The role of the AA-based framework in solving Robust Optimization problems

The definition of a formal connection between the AA-based optimization and robust optimization is not a trivial task, although these two paradigms seems to be characterized by several common features, and can be also considered as particular instances of the Granular Computing theory, which is an advanced tool for uncertainty management in optimization problems based on the holistic integration of multiple and heterogeneous paradigms of computational intelligence and information science [R2].

Roughly speaking, the general problem of robust optimization can be stated as follow:

$$\begin{aligned} \min_{\mathbf{x},\mathbf{u}} \quad & f_{obj}(\mathbf{x}, \mathbf{u}, \mathbf{p}) \\ \text{s.t.} \quad & \mathbf{g}(\mathbf{x}, \mathbf{u}, \mathbf{p}) \leq \mathbf{b} \\ & \mathbf{h}(\mathbf{x}, \mathbf{u}, \mathbf{p}) = \mathbf{c} \end{aligned} \tag{16}$$

where $\mathbf{u}$ is the vector of the control variables, $\mathbf{x}$ is the vector of the state variables, $\mathbf{p}$ is the vector of the uncertain parameters, f_{obj} is the objective function, $\mathbf{h}$ is the vector of the equality constraint functions, and $\mathbf{g}$ is the vector of the inequality constraint functions.

In robust optimization, which could be considered as a particular instance of probabilistic-scenario based programming, this problem is solved by defining the most relevant scenarios, which are characterized by a combination of crisp values of the uncertain parameters $\mathbf{p}$, and relaxing the problem constraints, by defining an in-feasibility penalty function, which measure the amount of constraint violation.

The proposed AA-based framework deploys a different paradigm to solve the problem in (R2). The main idea is to represent the uncertain parameters p by affine forms, and to compute the deterministic values

of the control variables, jointly with the corresponding affine forms of the state variables, by solving the following approximate optimization problem:

$$\begin{aligned} \min_{\mathbf{x},\mathbf{u}} \quad & \hat{f}_{obj}(\mathbf{x},\hat{\mathbf{u}},\hat{\mathbf{p}}) \\ \text{s.t.} \quad & \hat{\mathbf{g}}(\mathbf{x},\hat{\mathbf{u}},\hat{\mathbf{p}}) \leq \mathbf{b} \\ & \hat{\mathbf{h}}(\mathbf{x},\hat{\mathbf{u}},\hat{\mathbf{p}}) = \mathbf{c} \end{aligned} \tag{17}$$

where the objective function can be defined so that it measures the impact of the control variables on the bounds of the power system state variables, which are described by affine forms.

Such a formulation allows identifying the central values and the partial deviations of both the state and the control variables, satisfying the optimality conditions defined by the following Theorem:

Theorem 1 (AA-Optimality Conditions). [33] *Given an AA-based Optimization Problem as (17), $\hat{\boldsymbol{x}}^*$ is said to be an optimal solution if the quantity*

$$\left[\text{mid}\left(f_{obj}(\hat{\boldsymbol{x}})\right),\ \text{rad}\left(f_{obj}(\hat{\boldsymbol{x}})\right)\right]$$

has a minimum in $\hat{\boldsymbol{x}} = \hat{\boldsymbol{x}}^*$.

Hence, the optimality conditions in the AA domain can be satisfied by solving a deterministic multi-objective optimization problem, which can be solved by traditional methodologies, identifying a proper trade off between the two objective functions. Alternatively, in the scientific literature the chance to solve the problem by formulating a two stage decomposition has been described, by finding first the solution of the "nominal" problem, i.e. identifying the central values of the optimal affine forms without taking into account the uncertainties, and then the "perturbed" problem, considering the uncertainty. It is worth nothing that the latter problem requires the identification of a very large set of variables to be optimized, i.e. of (number of uncertainty sources)x(number of "uncertain quantities" to be optimized), increasing the problem cardinality.

3.2. Proposed Solution

The solution of the W-OPF problem formalized in (2) in the presence of data uncertainty can be effectively addressed by AA-based computing. To this aim, the state and control variables can be described by the following affine forms:

$$\hat{\mathbf{x}} = [\mathbf{P}^1_{gen},\ldots,\mathbf{P}^{N_{err}}_{gen},\mathbf{Q}^1_{gen},\ldots,\mathbf{Q}^{N_{err}}_{gen},\mathbf{V}^1_m,\ldots,\mathbf{V}^{N_{err}}_m] \tag{18}$$

and the uncertain optimization problem can be recasted in the affine domain as follows:

$$\begin{aligned} \min_{\hat{\mathbf{x}}} \quad & \hat{f}_{obj}(\hat{\mathbf{x}}) & \\ \text{s.t.} \quad & V_i^{min} \leq \hat{V}_i \leq V_i^{max} & \forall i \in [1,\ldots,N] \\ & P^{min}_{gen,i} \leq \hat{P}_{gen,i} \leq P^{max}_{gen,i} & \forall i \in \{PV;V\theta\} \\ & Q^{min}_{gen,i} \leq \hat{Q}_{gen,i} \leq Q^{max}_{gen,i} & \forall i \in \{PV;V\theta\} \\ & \hat{T}_k < T_k^{max} & \forall k \in [1,\ldots,N_l] \\ & \hat{P}^{fix}_{inj,i} = \hat{V}_i \sum_{j=1}^{N} \hat{V}_j\, y_{ij}\, \cos(\theta_{ij} + \hat{\delta}_j - \hat{\delta}_i) & \forall i \in [1,\ldots,N] \\ & \hat{Q}^{fix}_{inj,i} = \hat{V}_i \sum_{j=1}^{N} \hat{V}_j\, y_{ij}\, \sin(\theta_{ij} + \hat{\delta}_j - \hat{\delta}_i) & \forall i \in [1,\ldots,N] \\ & \hat{T}_k = \hat{T}_s + \frac{1}{mC_p}\int_{t_s}^{t_f} \left(q_s + \hat{I}_k^2\, R(\hat{T}_k) - \hat{q}_c - q_r\right) d\tau & \forall k \in [1,\ldots,N_l] \end{aligned} \tag{19}$$

This formulation of the W-OPF problem is strengthen, since it allows to directly deal with the affine forms of the state and control variables. Furthermore, this formulation allows to meld the shared uncertainty sources that plays roles in both the electric and thermal part of the problem, producing robust results in terms of conductor temperature estimation and optimal control variables identification. Eventually, this formulation allows to consider also further sources of uncertainties deriving from other phenomena of particular applications and that can be simply correlated to the other variables involved in the process.

The solution of this problem, which is defined in the AA mathematical domain, require the formulation of its robust counterpart in order to be solved by traditional algorithms. Based on Theorem 1, the robust counterpart of the OPF problem formulated in Eq. 19 can be constructed as a multi-objective NLP problem whose objective functions aim at minimizing both the central value and the radius of the original affine figure of merit, $\hat{f}_{obj}$, to be minimized.

All algebraic equations representing linear and non-linear equality constraints have to be solved by opportune operators defined in[24] which assess that two affine forms are equal if both their central values and all partial deviation assume the same value. Inequality constraints are also managed through opportune operators defined in[24] whose aim is to produce robust limitation of the considered quantity. For example, solving:

$$\hat{P}^{fix}_{inj,i} = \hat{P}^{calc}_{inj,i} \tag{20}$$

needs to impose:

$$\begin{aligned} P^{fix,0}_{inj,i} &= P^{calc,0}_{inj,i} \\ P^{fix,1}_{inj,i} &= P^{calc,1}_{inj,i} \\ &\vdots \\ P^{fix,Nerr}_{inj,i} &= P^{calc,Nerr}_{inj,i} \end{aligned} \tag{21}$$

and solving:

$$\hat{T}_k < T^{max}_k \tag{22}$$

needs to require:

$$\sup(\hat{T}_k) < T^{max}_k \tag{23}$$

Hence,the problem to be solved is:

$$\begin{aligned} \min_{\hat{\mathbf{x}}} \quad & [mid\big(\hat{f}_{obj}(\hat{\mathbf{x}})\big);\ sup\big(\hat{f}_{obj}(\hat{\mathbf{x}})\big)] \\ \text{s.t.} \quad & V^{min}_i \le \inf\left(\hat{V}_i\right) \le \sup\left(\hat{V}_i\right) \le V^{max}_i && \forall i \in [1,\dots,N] \\ & P^{min}_{gen,i} \le \inf\left(\hat{P}_{gen,i}\right) \le \sup\left(\hat{P}_{gen,i}\right) \le P^{max}_{gen,i} && \forall i \in \{PV; V\theta\} \\ & Q^{min}_{gen,i} \le \inf\left(\hat{Q}_{gen,i}\right) \le \sup\left(\hat{Q}_{gen,i}\right) \le Q^{max}_{gen,i} && \forall i \in \{PV; V\theta\} \\ & \sup(\hat{T}_k) < T^{max}_k && \forall k \in [1,\dots,N_l] \\ & \hat{P}^{fix,c}_{inj,i} = \hat{P}^{calc,c}_{inj,i} && \forall i \in [1,\dots,N],\ \forall c \in [1,\dots,N_{err}] \\ & \hat{Q}^{fix,c}_{inj,i} = \hat{Q}^{calc,c}_{inj,i} && \forall i \in [1,\dots,N],\ \forall c \in [1,\dots,N_{err}] \end{aligned} \tag{24}$$

where:

$$\hat{P}^{calc}_{inj,i} = \hat{V}_i \sum_{j=1}^{N} \hat{V}_j\, y_{ij}\, \cos(\theta_{ij} + \hat{\delta}_j - \hat{\delta}_i) \qquad \forall i \in [1,\dots,N]$$

$$\hat{Q}^{calc}_{inj,i} = \hat{V}_i \sum_{j=1}^{N} \hat{V}_j\, y_{ij}\, \sin(\theta_{ij} + \hat{\delta}_j - \hat{\delta}_i) \qquad \forall i \in [1,\dots,N]$$

$$\hat{T}_k = \hat{T}_s + \frac{1}{mC_p} \int_{t_s}^{t_f} \big(q_s + \hat{I}^2_k\, R(\hat{T}_k) - \hat{q}_c - q_r\big) d\tau \qquad \forall k \in [1,\dots,N_l]$$

Line	From	To	Length $[Km]$	Line Resistance r $[p.u.]$	Line Reactance x $[p.u.]$	Line Susceptance b $[p.u.]$
1	1	2	33.20	0,00821	0,056278	0,02223
2	2	3	3.42	0,000846	0,005797	0,00229
3	1	3	34.7	0,008581	0,05882	0,023234
4	3	9	≈ 10	0,002473	0,016951	0,006696
5	8	9	≈ 10	0,002473	0,016951	0,006696
6	2	10	10.2	0,002522	0,01729	0,00683
7	2	7	16	0,003957	0,027122	0,010713
8	6	7	≈ 1.7	0,00042	0,002882	0,001138
9	5	6	≈ 1.7	0,00042	0,002882	0,001138
10	4	5	10.8	0,002671	0,018307	0,007231

Table 2: Branch Data

4. Case Study

The proposed methodology have been applied in the task of solving a W-OPF problem for a real case study, which is based on a congested transmission network characterized by a massive pervasion of wind generators. The analyzed 10-buses power system is represented in Fig. 1 and characterized by the data summarized in Tabs. 3 and 2. In this study, both the generators and the loads are assumed to operate at constant power factor.

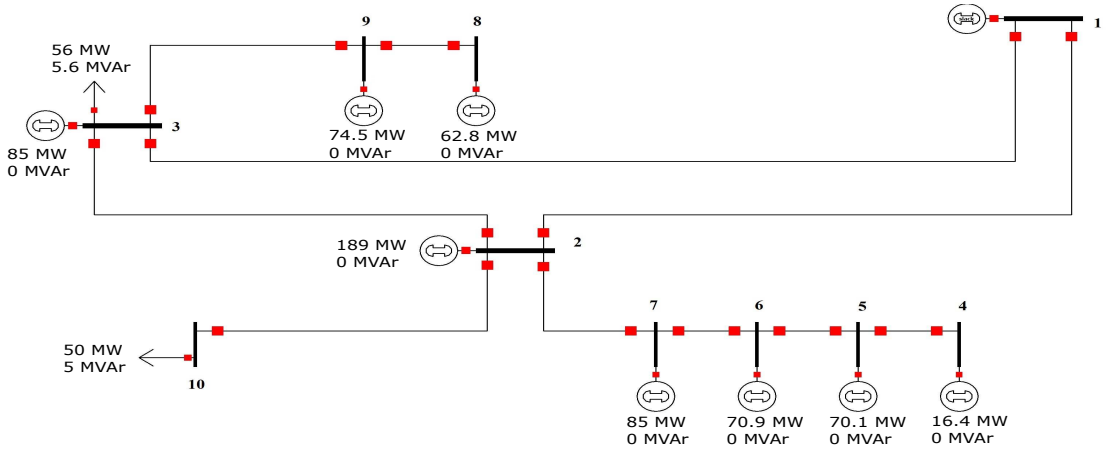

Figure 1: The Analyzed Power System

The analyzed power system is a strategic section of the transmission network, since it collects a large amount of the total wind energy generated in the served area, and it is frequently congested, especially during high windy periods. To mitigate the consequences of these critical conditions, the TSO imposes severe power curtailments to all wind generators, which modify the "natural" market equilibrium. Hence, more effective loading strategies aimed at reliably increasing the components exploitation are particularly useful in this context, in order to allow TSO to reduce the wind power curtailments, enhancing the network flexibility.

4.1. Uncertain-OPF

The first case study analyzed is based on the application of the AA-based methodology in the task of solving an uncertain OPF problem by considering all the loads varying in a 20% nominal power radius interval, and the wind speed varying on a 5% with respect to its forecasted value[34]. These uncertain sources are represented by two independent noise symbols, one for the load's and one for the wind generation's profiles.

Bus	Type	P_d $[MW]$	Q_d $[MVAr]$	P_g $[MW]$	Q_g $[MVAr]$
1	Slack	0	0	0	0
2	Wind Generator	0	0	189	0
3	Wind Generator	56	5.6	85	0
4	Wind Generator	0	0	16.4	0
5	Wind Generator	0	0	70.1	0
6	Wind Generator	0	0	70.9	0
7	Wind Generator	0	0	85	0
8	Wind Generator	0	0	62.8	0
9	Wind Generator	0	0	74.5	0
10	Load	50	5	/	/

Table 3: Bus Data

In particular, the wind speed is modeled by the following affine form:

$$\hat{v}_w = v_w^{for} + 0.05\ v_w^{for}\ \epsilon_1 + 0\ \epsilon_2 \tag{25}$$

Once uncertainty in wind speed is modeled, its propagation into the wind power outputs has to be modeled in order to perform the W-OPF analysis. This is done by modeling each wind farm through an equivalent power curve fitted on real data acquired form wind farms in the considered area[35].

Starting from these power curves, the lower and upper bounds of the generated wind power are computed considering the wind power output bounds associated to wind speed bounds, through the aforementioned polynomial power curve model denoted with $PC(P_{g,i}^{nom}, v_s)$ in the following expressions:

$$\begin{aligned} P_{g,i}^{inf} &= PC(P_{g,i}^{nom}, v_s^{inf}) \\ P_{g,i}^{sup} &= PC(P_{g,i}^{nom}, v_s^{sup}) \end{aligned} \tag{26}$$

These bounds translate in the AA domain in a central value and a partial deviation which is associated to the error symbol proper of the uncertainty in wind speed, as shown in the following:

$$P_{g,i}^0 = \frac{P_{g,i}^{inf} + P_{g,i}^{sup}}{2}$$

$$P_{g,i}^1 = \frac{P_{g,i}^{sup} - P_{g,i}^{inf}}{2}$$

Finally, the affine forms of the generated wind power are defined as:

$$\hat{P}_{g,i} = P_{g,i}^0 + P_{g,i}^1\ \epsilon_1 \tag{27}$$

As far as the load uncertainty is concerned, the active and reactive power demand at the i^{it} bus can be defined as:

$$\begin{aligned} \hat{P}_{d,i} &= P_{d,i}^{nom} + 0.1\ P_{d,i}^{nom}\ \epsilon_2 \\ \hat{Q}_{d,i} &= Q_{d,i}^{nom} + 0.1\ Q_{d,i}^{nom}\ \epsilon_2 \end{aligned}$$

To identify the minimum power curtailments that assure a secure and reliable power system operation, the following uncertain OPF can be solved:

$$
\begin{aligned}
\min_{\mathbf{x}} \quad & \sum_{i=1}^{N_{GEN}} \mathrm{mid}(\hat{P}^2_{cut,i}) + \sup(\hat{P}^2_{cut,i}) \\
\text{s.t.} \quad & V_i^{min} \leq \inf\left(\hat{V}_i\right) \leq \sup\left(\hat{V}_i\right) \leq V_i^{max} && \forall\, i \in [1,\ldots,N] \\
& I_k < I_k^{max} && \forall\, k \in [1,\ldots,N_l] \\
& P^{calc,n}_{inj,i} = P^{fix,n}_{inj,i} && \forall i \in \{PV;\ PQ\},\ \forall n \in [1,\ldots,N_{err}] \\
& Q^{calc,n}_{inj,i} = Q^{fix,n}_{inj,j} && \forall i \in \{PQ\},\ \forall n \in [1,\ldots,N_{err}] \\
& \hat{P}^{calc}_{inj,i} = \hat{V}_i^{Re} \sum_{j=1}^{N} \left(G_{i,j}\hat{V}_j^{Re} - B_{i,j}\hat{V}_j^{Im}\right) + \hat{V}_i^{Im} \sum_{j=1}^{N} \left(B_{i,j}\hat{V}_j^{Re} + G_{i,j}\hat{V}_j^{Im}\right) && \forall i \in \{PV;\ PQ\} \\
& \hat{Q}^{calc}_{inj,i} = \hat{V}_i^{Im} \sum_{j=1}^{N} \left(G_{i,j}\hat{V}_j^{Re} - B_{i,j}\hat{V}_j^{Im}\right) - \hat{V}_i^{Re} \sum_{j=1}^{N} \left(B_{i,j}\hat{V}_j^{Re} + G_{i,j}\hat{V}_j^{Im}\right) && \forall i \in \{PQ\}
\end{aligned}
\tag{28}
$$

where the decision variables are described by the following affine forms:

$$
\mathbf{x} = [\mathbf{P}_0^{cut}, \mathbf{P}_1^{cut}, \ldots, \mathbf{P}_{N_{err}}^{cut} \mathbf{V}_0^{Re}, \mathbf{V}_1^{Re}, \ldots, \mathbf{V}_{N_{err}}^{Re}, \mathbf{V}_0^{Im}, \mathbf{V}_1^{Im}, \ldots, \mathbf{V}_{N_{err}}^{Im}] \tag{29}
$$

This problem has been solved in Matlab ®, by using the embedded optimization solvers. The effectiveness of the computed solution has been assessed by comparing the obtained results with those obtained by applying a Monte Carlo simulation on a particular case whose principal input parameter are shown in Tab. 4.

Wind Speed	10	$[m/s]$
Wind Direction	226	deg
Environmental Temperature	5.52	℃
hour	14	
day	April 8th	

Table 4: Case Study Data

Wind Speed 5% uncertainty in wind speed forecasting translate into generated power whose bounds are:

Bus #	Lower Bound [MW]	Upper Bound [MW]
1	0	0
2	121.3994	158.9741
3	54.5976	71.4963
4	10.5341	13.7946
5	45.0270	58.9634
6	45.5408	59.6363
7	54.5976	71.4963
8	40.3380	52.8231
9	47.8532	62.6644
10	0	0

Table 5: Forecasted Wind Generation

Load has been considered varying 20% from its forecasted value, bringing to a ratio between the generated and consumed power which is in the interval [3.30 6.48].

In the following, Fig. 2 reports the wind power curtailment bounds for each network buses, which is a strategic information extremely useful in solving many critical operation problems, such as robust reserve scheduling, and optimal energy storage operation. Another important information derived from the obtained affine forms is the quantification of the impacts of each uncertainty sources on the problem solutions. This is clearly shown in Tab. 6, where the central values and the partial deviations of the wind power curtailments

have been reported. This information has a great impact on power system operation, providing useful information aimed at supporting the operator in solving complex decision making problems. Moreover, once the uncertainty levels are defined, the proposed framework provides the boundary profiles of both the state (see Tab. 9, 10) and control (see Fig. 3 and Tab. 7, 8) variables, which are useful for assessing the robustness of the computed set-points.

Another valuable feature of the AA-based method is that it allows to overcome the limitation of classical IA-based computing, avoiding error explosion phenomena and estimating solution bounds, which are consistent with respect to the ones obtained by the Monte Carlo procedures.

A theoretical explanation of these results can be provided by reminding that the AA method is a particular type of a self-validated computing, since it uses ranges, rather than distributions, to describe the data uncertainty. Specifically, the affine form $\hat{z} = \hat{f}(\hat{x}) = z_0 + \sum_{h=1}^{p} x_h \epsilon_h$ defines a range $[z_0 - \sum_{h=1}^{p} |z_h|;\ z_0 + \sum_{h=1}^{p} |z_h|]$ for the variable z, namely a set of real values that is guaranteed to contain the true value of z, provided that the input variable x lies in the range $[x_0 - \sum_{h=1}^{p} |x_h|;\ x_0 + \sum_{h=1}^{p} |x_h|]$. This property, which is referred to as the "fundamental invariant of range analysis", can be generalized as follows [32]:

Theorem 2 (Fundamental Invariant of Range Analysis). *For every function $f : \Re^n \rightarrow \Re^m$, it is possible to define an AA-based range extension, f^A, with the following property:*

*If the input vector $(x_1, \ldots, x_n)$ lies in the range jointly determined by the given affine forms $(\hat{x}_1, \ldots, \hat{x}_n)$, namely $x_j \in [x_{j,0} - \sum_{h=1}^{p} |x_{j,h}|;\ x_{j,0} + \sum_{h=1}^{p} |x_{j,h}|]\ \forall j \in [1, n]$, then the quantities $(z_1, \ldots, z_n) = f(x_1, \ldots, x_n)$ are **guaranteed** to lie in the range jointly defined by the affine forms $(\hat{z}_1, \ldots, \hat{z}_n) = f(\hat{x}_1, \ldots, \hat{x}_n)$*

The overestimation, and hence the conservative nature of the determination of the joint range obtained by the affine forms $(\hat{z}_1, \ldots, \hat{z}_n)$, depends on the computing paradigm adopted to estimate f^A , which is selected on the basis of a proper trade-off between accuracy and computational burden. This is confirmed for the analysis presented in this paper through a comparison with a Monte Carlo model, which is assumed to give the best inner approximation of the solution bounds, as the bounds obtained by the presented AA-based W-OPF method are slightly conservative (please see Figures 2-4).

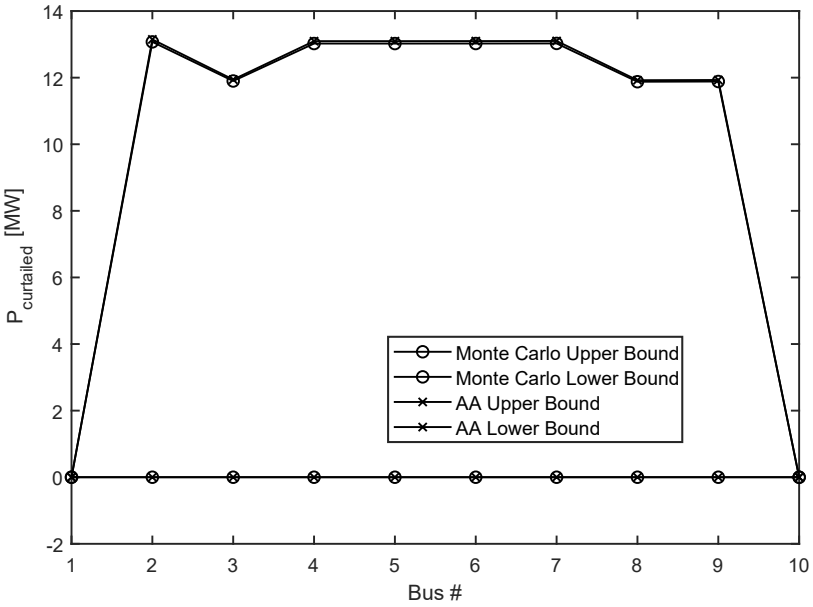

Figure 2: Wind Power Curtailment - Bounds

Bus #	Central Value	Error Symbol 1	Error Symbol 2
1	0	0	0
2	6,574241	1,410193	-5,16405
3	5,971402	0,067399	-5,904
4	6,548054	6,53676	-0,01129
5	6,548129	6,534076	-0,01405
6	6,549027	6,546217	-0,00281
7	6,550674	5,166902	-1,38377
8	5,96145	5,869529	-0,09192
9	5,964621	5,79769	-0,16693
10	0	0	0

Table 6: Affine Form - P_{cut}

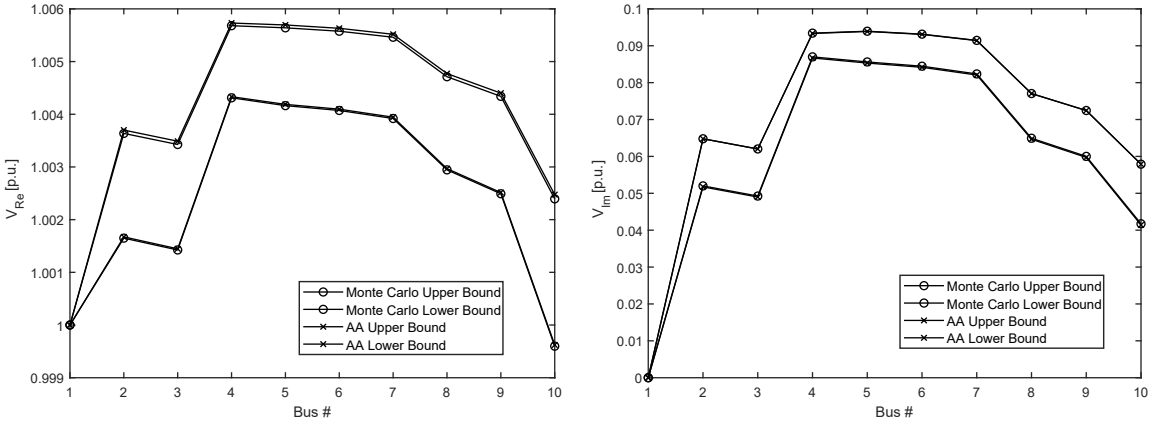

Figure 3: Voltage Real and Imaginary Parts - Bounds

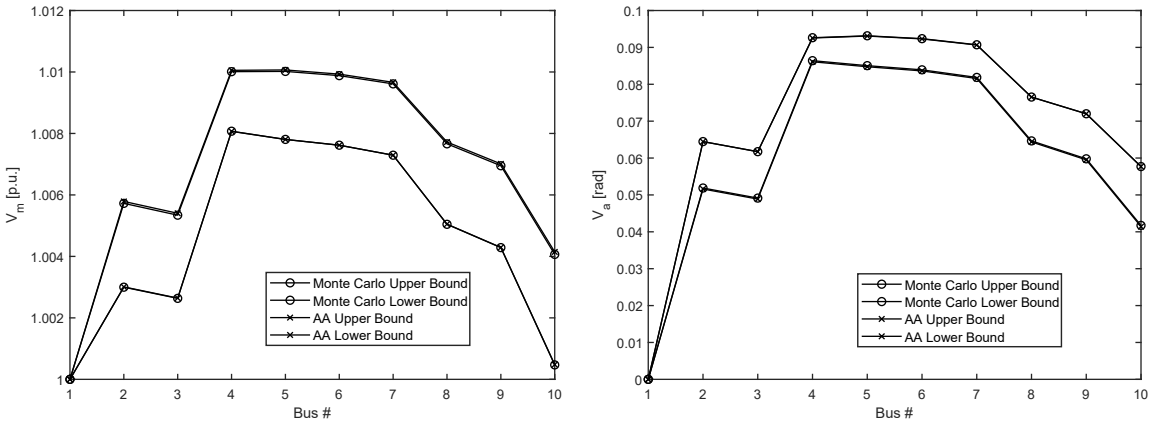

Figure 4: Voltage Magnitudes and Angles - Bounds

Bus #	Central Value	Error Symbol 1	Error Symbol 2
1	1	0	0
2	1,002686	0,000241	-0,00077
3	1,002468	0,000239	-0,00078
4	1,005032	7,85E-06	-0,00069
5	1,004941	6,16E-05	-0,00069
6	1,004864	7,36E-05	-0,00069
7	1,004731	8,94E-05	-0,0007
8	1,00387	0,00016	-0,00074
9	1,003458	0,000189	-0,00075
10	1,001049	0,000277	-0,00115

Table 7: Affine Form - V_r

Bus #	Central Value	Error Symbol 1	Error Symbol 2
1	0	0	0
2	0,058258	0,004201	-0,00232
3	0,055501	0,004146	-0,00237
4	0,090017	1,42E-03	-0,00191
5	0,089593	2,37E-03	-0,00191
6	0,088622	2,55E-03	-0,00191
7	0,086734	2,75E-03	-0,00192
8	0,070842	0,003893	-0,0023
9	0,066085	0,004034	-0,00232
10	0,049658	0,004198	-0,00404

Table 8: Affine Form - V_i

Bus #	Central Value	Error Symbol 1	Error Symbol 2	Approximation Error
1	-1,95033	-0,14329	0,083664	0
2	0,957644	0,137521	0,05164	0,000274
3	-0,15946	0,067516	-0,05296	0,000199
4	0,023321	-5,22E-02	0,000113	5,15E-05
5	0,314092	-9,10E-03	0,000141	9,86E-06
6	0,318415	-8,58E-03	2,81E-05	9,49E-06
7	0,394746	1,65E-02	0,013838	3,75E-05
8	0,280431	-0,00831	0,000919	1,50E-05
9	0,343752	0,00179	0,001669	1,67E-05
10	-0,5	-1,67E-17	-0,1	0,000219

Table 9: Affine Form - P_{calc}

Bus #	Central Value	Error Symbol 1	Error Symbol 2	Approximation Error
1	0,172101	0,012562	0,014823	0
2	5,27E-15	-1,27E-16	8,50E-17	0,001215
3	-0,056	2,28E-14	-0,0112	0,000772
4	2,31E-13	3,68E-13	-4,55E-15	1,69E-04
5	1,29E-14	-6,91E-14	1,79E-16	4,06E-05
6	1,74E-13	-1,62E-13	-2,90E-15	3,96E-05
7	1,91E-13	2,58E-13	3,74E-15	1,38E-04
8	-1,46E-13	-1,78E-13	5,41E-14	5,88E-05
9	1,33E-12	3,18E-12	5,03E-14	2,05E-05
10	-0,05	-7,81E-18	-0,01	0,000818

Table 10: Affine Form - Q_{calc}

4.2. Uncertain W-OPF

In order to assess the benefits deriving by the application of a dynamic loading strategy, the power line connecting the buses 1 and 2 have been equipped by a DTR system, which acquires the conductor temperature and the environmental variables in the expected critical span, and the corresponding static loading limit has been converted in a dynamic thermal constrain. In this case, the control variables are described by the following affine forms:

$$\mathbf{x} = [\mathbf{P}_0^{cut}, \mathbf{P}_1^{cut}, \ldots, \mathbf{P}_{N_{err}}^{cut} \mathbf{V}_0^{Re}, \mathbf{V}_1^{Re}, \ldots, \mathbf{V}_{N_{err}}^{Re}, \mathbf{V}_0^{Im}, \mathbf{V}_1^{Im}, \ldots, \mathbf{V}_{N_{err}}^{Im}] \tag{30}$$

and the overall W-OPF problem can be formulated as:

$$\begin{aligned}
\min_{\mathbf{x}} \quad & \sum_{i=1}^{N_{GEN}} \text{mid}(\hat{P}_{cut,i}^2) + \sup(\hat{P}_{cut,i}^2) & \\
\text{s.t.} \quad & V_i^{min} \leq \inf\left(\hat{V}_i\right) \leq \sup\left(\hat{V}_i\right) \leq V_i^{max} & \forall\, i \in [1, \ldots, N] \\
& T_k < T_k^{max} & \forall\, k \in [1, \ldots, N_l] \\
& P_{inj,i}^{calc,n} = P_{inj,i}^{fix,n} & \forall i \in \{PV;\ PQ\},\ \forall n \in [1, \ldots, N_{err}] \\
& Q_{inj,i}^{calc,n} = Q_{inj,j}^{fix,n} & \forall i \in \{PQ\},\ \forall n \in [1, \ldots, N_{err}] \\
& \hat{P}_{inj,i}^{calc} = \hat{V}_i^{Re} \sum_{j=1}^{N} \left(G_{i,j}\hat{V}_j^{Re} - B_{i,j}\hat{V}_j^{Im}\right) + \hat{V}_i^{Im} \sum_{j=1}^{N} \left(B_{i,j}\hat{V}_j^{Re} + G_{i,j}\hat{V}_j^{Im}\right) & \forall i \in \{PV;\ PQ\} \\
& \hat{Q}_{inj,i}^{calc} = \hat{V}_i^{Im} \sum_{j=1}^{N} \left(G_{i,j}\hat{V}_j^{Re} - B_{i,j}\hat{V}_j^{Im}\right) - \hat{V}_i^{Re} \sum_{j=1}^{N} \left(B_{i,j}\hat{V}_j^{Re} + G_{i,j}\hat{V}_j^{Im}\right) & \forall i \in \{PQ\} \\
& T_k = T_s + \frac{1}{mC_p} \int_{t_s}^{t_f} \left(q_s + I_k^2\, R(T_k) - q_c - q_r\right) d\tau & \forall\, k \in [1, \ldots, N_l]
\end{aligned} \tag{31}$$

The obtained results have been summarized in Figs. 5-6 and in Tab. 11. By analyzing these data it is worth observing the benefits deriving by the deployment of the AA-based W-OPF analysis, which allows lowering the wind power curtailments, assuring the system security also for the worst-case instance of the uncertain variables.

Bus #	Central Value	Error Symbol 1	Error Symbol 2
1	0	0	0
2	4,866667	2,998339	-1,86833
3	5,385078	5,384418	-0,00066
4	4,846931	4,606996	-0,23993
5	4,847203	4,602754	-0,24445
6	4,847295	4,583567	-0,26373
7	4,849383	4,563162	-0,28622
8	5,373174	5,29919	-0,07398
9	5,376808	5,226771	-0,15004
10	0	0	0

Table 11: P_{cut} - Dynamic Thermal Rating

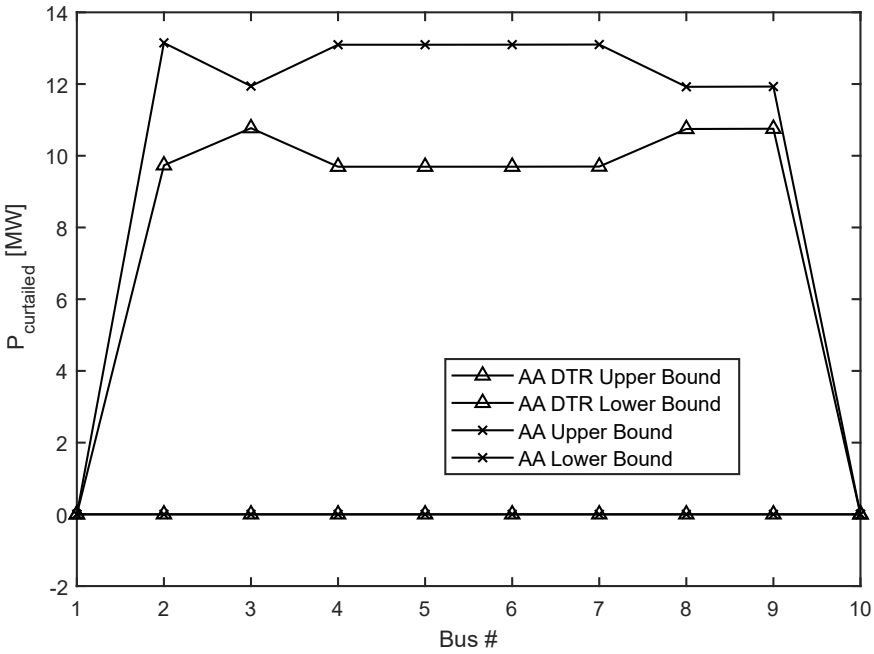

Figure 5: P_{cut} - Dynamic Thermal Rating vs Static Rating

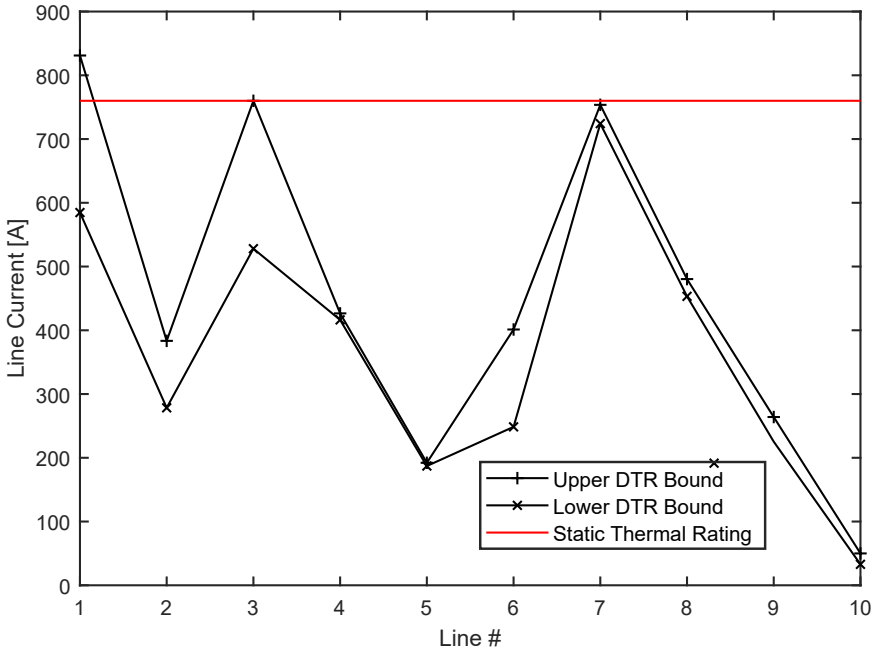

Figure 6: Line Currents - Dynamic Thermal Rating vs Static Rating Limit

The computational burdens of the analyzed techniques are summarized in Tab. 12, which reports the simulation times observed during the studies.

	Elapsed Time [sec]
Traditional OPF	1.2
AA-Based OPF - STR	3.5
AA-Based OPF - DTR	4.5

Table 12: Simulations Elapsed Time

Finally, the results of a day of operation has been shown in Fig. 7 and Fig. 8-9. In particular, Fig. 7 show the upper bound of the overall curtailment profiles in case of STR and DTR, demonstrating the effectiveness of the proposed methodology in reducing the power curtailment of wind farm by increasing the capability of a congested line.

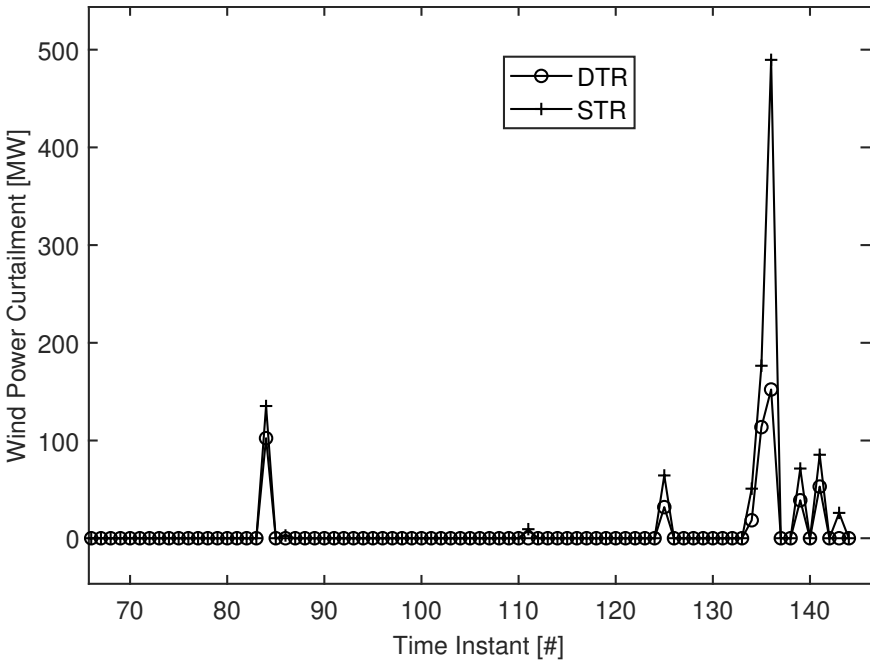

Figure 7: Dynamic Thermal Rating vs Static Thermal Rating

Moreover Fig. 8 and 9 depict the overall power curtailment profile joint to the wind speed and environmental temperature profiles.

It is important to highlight that the results have been obtained considering the conductor temperature equal to its maximum value at each time instant. This means that the heat capacity of the conductor has been not considered in the computation of the thermal constraints. Hence, only the more favorable cooling conditions of the conductor contributes to the exploitation of the additional capability of the line operated under DTR regime.

The presented analysis is related to a relatively simple test system, whose size, configuration and characteristics are all taken from a real network, in order to correctly represent analyzed section of actual transmission system with a high penetration level of wind generation. The previous work by the authors was aimed at assessing the effectiveness of the AA-based methodology for solving large and very large power networks, e.g. [25], suggesting that the AA-based W-OPF analysis presented in this paper can be also applied in case of larger networks, characterized by multiple congested power lines, massive penetration of renewable power generators, distributed composite loads, and complex market dynamics. The authors are currently working on this problem.

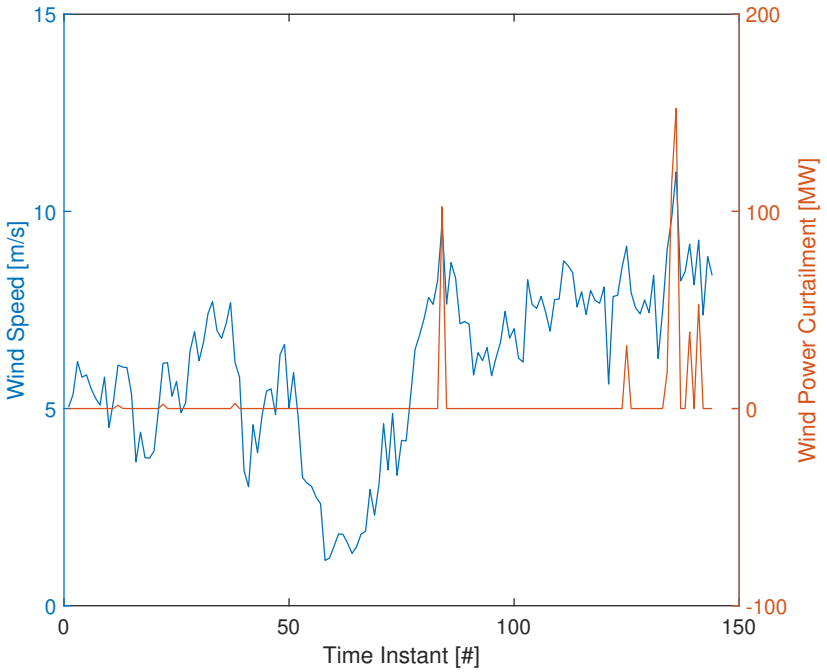

Figure 8: Wind Speed vs Wind Power Curtailment

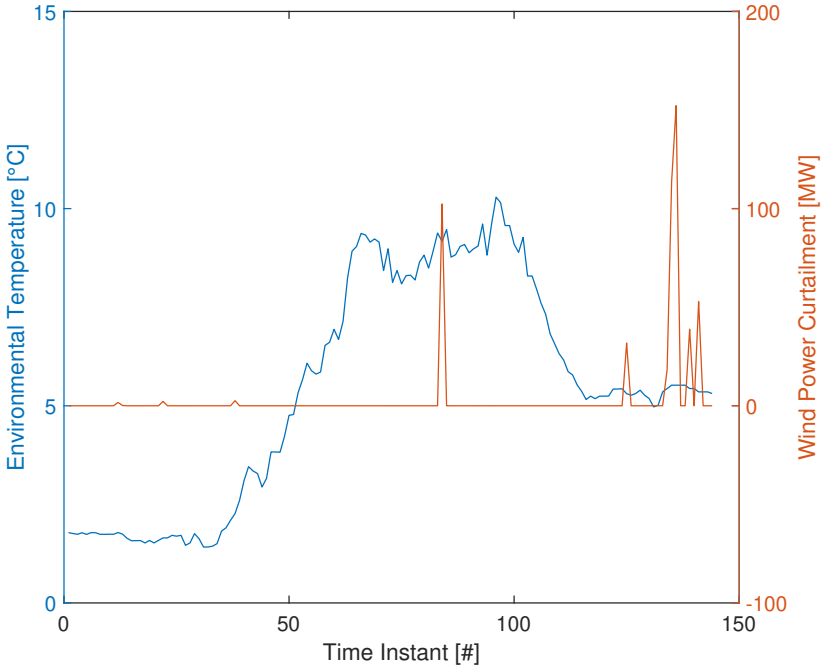

Figure 9: Environmental Temperature vs Wind Power Curtailment

5. Conclusions and Future Works

Weather-based optimal power flow is one of the most promising enabling methodologies aimed at improving the hosting capacity of renewable power generators, the power components exploitation, and the network flexibility, without requiring the need for new electrical infrastructures. Anyway, its large-scale deployment in realistic operation scenario could be hindered by the multiple and correlated uncertainties affecting both the generated/demanded power profiles, and the components thermal modeling, which should be accurately represented and managed in order to obtain reliable problem solutions, satisfying the severe security and reliability levels characterizing modern power system operation. To address these challenging issues this paper:

- conceptualized a reliable solution technique based on AA, which allowed solving uncertain W-OPF analysis by explicitly considering the effects of the load/generator uncertainty and the components' thermal dynamics on both the objective function and the power system constraints;
- proposed a new computing model based on the range analysis theory, which aims at propagating the effects of the wind speed uncertainty into the generated power;
- presented and discussed the results obtained on a real case study, which was based on a congested portion of a real transmission system characterized by a massive pervasion of wind generators.

The analysis of the obtained experimental results demonstrated the effectiveness of the AA-based computing paradigm in reliably identifying the bounds of the uncertain W-OPF problem solutions, by considering all the possible combinations of the input data uncertainty. This result is still more relevant if we consider that the affine form of the problem solution has been quickly obtained by solving a deterministic optimization problem, which has been formalized according to proper AA-based mathematical operators.

As mentioned in the paper, an important advantage of the presented AA-based method is that it allows to obtain, in one relatively simple calculation step, the lower and upper boundaries (i.e. the best and the worst case estimations) of the problem solution, instead of performing a large number of probabilistic Monte Carlo runs, which are required to capture these bounds from the tails of output distributions. However, the AA-based solution might return unrealistically large ranges when the probabilities around the boundary values are very small. To resolve that issue, a suitable confidence interval can be introduced for selecting the input uncertainty ranges, which can be obtained either from an assumed distribution of uncertainties around the central (or most expected) value, or from a limited number of Monte Carlo runs. The authors are currently investigating this problem as a possible future direction for improving the presented analysis.

References

[1] G. Pepermans, J. Driesen, D. Haeseldonckx, R. Belmans, W. D'haeseleer, Distributed Generation: Definition, Benefits and Issues, Energy policy 33 (6) (2005) 787–798.

[2] K. G. Boroojeni, M. H. Amini, S. Iyengar, M. Rahmani, P. M. Pardalos, An economic dispatch algorithm for congestion management of smart power networks, Energy Systems 8 (3) (2017) 643–667.

[3] E. M. Carlini, C. Pisani, A. Vaccaro, D. Villacci, Dynamic Line Rating Monitoring in WAMS: Challenges and Practical Solutions, in: 2015 IEEE 1st International Forum on Research and Technologies for Society and Industry Leveraging a better tomorrow (RTSI), 2015, pp. 359–364. doi:10.1109/RTSI.2015.7325124.

[4] C. J. Wallnerström, Y. Huang, L. Söder, Impact from Dynamic Line Rating on Wind Power Integration, IEEE Transactions on Smart Grid 6 (1) (2015) 343–350.

[5] G. Coletta, A. Vaccaro, D. Villacci, A Review of the Enabling Methodologies for PMUs-Based Dynamic Thermal Rating of Power Transmission Lines, Electric Power Systems Research 152 (2017) 257–270.

[6] M. Nick, O. A. Mousavi, R. Cherkaoui, M. Paolone, Integration of Transmission Lines Dynamic Thermal Rating into Real-Time Optimal Dispatching of Power Systems, in: Power Engineering Conference (UPEC), 2015 50th International Universities, IEEE, 2015, pp. 1–6.

[7] J. Cao, W. Du, H. Wang, Weather-Based Optimal Power Flow With Wind Farms Integration, IEEE Transactions on Power Systems 31 (4) (2016) 3073–3081.

[8] M. X. Wang, X. S. Han, Study on Electro-Thermal Coupling Optimal Power Flow Model and its Simplification, in: IEEE PES General Meeting, 2010, pp. 1–6. doi:10.1109/PES.2010.5589644.

[9] C. Pisani, A. Vaccaro, D. Villacci, Dynamic Line Rating of Overhead Lines by Cooperative and Self-Organizing Sensor Networks, in: 2015 AEIT International Annual Conference (AEIT), 2015, pp. 1–6. doi:10.1109/AEIT.2015.7415239.

[10] J. Shu, R. Guan, L. Wu, Optimal Power Flow in Distribution Network Considering Spatial Electro-Thermal Coupling Effect, IET Generation, Transmission Distribution 11 (5) (2017) 1162–1169. doi:10.1049/iet-gtd.2016.0909.
[11] A. I. SARWAT, M. AMINI, A. DOMIJAN, A. DAMNJANOVIC, F. KALEEM, Weather-Based Interruption Prediction in the Smart Grid Utilizing Chronological Data, Journal of Modern Power Systems and Clean Energy 4 (2) (2016) 308–315. doi:10.1007/s40565-015-0120-4.
URL https://doi.org/10.1007/s40565-015-0120-4
[12] A. I. Sarwat, A. Domijan, M. H. Amini, A. Damnjanovic, A. Moghadasi, Smart Grid reliability assessment utilizing Boolean Driven Markov Process and variable weather conditions, in: 2015 North American Power Symposium (NAPS), 2015, pp. 1–6. doi:10.1109/NAPS.2015.7335101.
[13] P. Zhang, S. T. Lee, Probabilistic Load Flow Computation Using the Method of Combined Cumulants and Gram-Charlier Expansion, IEEE Transactions on Power Systems 19 (1) (2004) 676–682. doi:10.1109/TPWRS.2003.818743.
[14] P. Wei, J. K. Liu, Q. Zhou, D. J. Wang, A Probabilistic Power Flow Algorithm Based on Semi-Variable and Series Expansion, in: 2017 IEEE 2nd International Conference on Big Data Analysis (ICBDA), 2017, pp. 563–567. doi:10.1109/ICBDA.2017.8078697.
[15] A. Schellenberg, W. Rosehart, J. Aguado, Cumulant-Based Probabilistic Optimal Power Flow (P-OPF) with Gaussian and Gamma Distributions, IEEE Transactions on Power Systems 20 (2) (2005) 773–781.
[16] G. Verbic, C. A. Canizares, Probabilistic Optimal Power Flow in Electricity Markets Based on a Two-Point Estimate Method, IEEE Transactions on Power Systems 21 (4) (2006) 1883–1893.
[17] G.-C. J. Sebastián, C.-L. J. Alexander, G.-E. Mauricio, Stochastic AC Optimal Power Flow Considering the Probabilistic Behavior of the Wind, Loads and Line Parameters, Ingeniería, Investigación y Tecnología 15 (4) (2014) 529–538.
[18] A. Mohapatra, P. Bijwe, B. Panigrahi, Optimal Power Flow with Multiple Data Uncertainties, Electric Power Systems Research 95 (Supplement C) (2013) 160 – 167. doi:https://doi.org/10.1016/j.epsr.2012.06.017.
[19] S. Peng, J. Tang, W. Wang, F. Liu, J. Zheng, An Unscented Transformation Based Probabilistic Power Flow for Studies on Uncertainty Sources in AC/DC Grid, in: 2017 IEEE International Conference on Smart Grid and Smart Cities (ICSGSC), 2017, pp. 221–226. doi:10.1109/ICSGSC.2017.8038580.
[20] J. Schwippe, O. Krause, C. Rehtanz, Probabilistic Load Flow Calculation based on an enhanced convolution technique, in: 2009 IEEE Bucharest PowerTech, 2009, pp. 1–6. doi:10.1109/PTC.2009.5281798.
[21] S. Patra, R. B. Misra, Probabilistic Load Flow Solution Using Method of Moments, in: 1993 2nd International Conference on Advances in Power System Control, Operation and Management, APSCOM-93., 1993, pp. 922–934 vol.2.
[22] A. B. Krishna, N. Gupta, K. R. Niazi, A. Swarnkar, Probabilistic Power flow in Radial Distribution Systems Using Point Estimate Methods, in: 2017 4th International Conference on Advanced Computing and Communication Systems (ICACCS), 2017, pp. 1–6. doi:10.1109/ICACCS.2017.8014677.
[23] L. Pereira, V. Da Costa, A. Rosa, Interval Arithmetic in Current Injection Power Flow Analysis, International Journal of Electrical Power and Energy Systems 43 (1) (2012) 1106–1113.
[24] A. Vaccaro, C. A. Canizares, D. Villacci, An Affine Arithmetic-Based Methodology for Reliable Power Flow Analysis in the Presence of Data Uncertainty, IEEE Transactions on Power Systems 25 (2) (2010) 624–632. doi:10.1109/TPWRS.2009.2032774.
[25] A. Vaccaro, C. A. Cañizares, An affine arithmetic-based framework for uncertain power flow and optimal power flow studies, IEEE Transactions on Power Systems 32 (1) (2017) 274–288.
[26] IEEE Standard for Calculating the Current-Temperature Relationship of Bare Overhead Conductors, IEEE Std 738-2012 (Revision of IEEE Std 738-2006 - Incorporates IEEE Std 738-2012 Cor 1-2013) (2013) 1–72doi:10.1109/IEEESTD.2013.6692858.
[27] A. Pavlinic, V. Komen, Direct Monitoring Methods of Overhead Line Conductor Temperature, Engineering Review : International journal for publishing of original researches from the aspect of structural analysis, materials and new technologies in the field of mechanical engineering, shipbuilding, fundamental engineering sciences, computer sciences, electrical engin 37 (2) (2017) 134–146.
[28] Study of the Monitorng Systems for Dynamic Line Rating, Energy Procedia 105 (2017) 2557 – 2562.
[29] R. Mai, L. Fu, X. HaiBo, Dynamic Line Rating estimator with synchronized phasor measurement, in: 2011 International Conference on Advanced Power System Automation and Protection, Vol. 2, 2011, pp. 940–945. doi:10.1109/APAP.2011.6180545.
[30] L. H. Figueiredo, J. Stolfi, Adaptive Enumeration of Implicit Surfaces with Affine Arithmetic, in: Computer Graphics Forum, Vol. 15, Wiley Online Library, 1996, pp. 287–296.
[31] J. Stolfi, L. De Figueiredo, An Introduction to Affine Arithmetic, Trends in Applied and Computational Mathematics 4 (3) (2003) 297–312.
[32] L. H. De Figueiredo, J. Stolfi, Affine Arithmetic: Concepts and Applications, Numerical Algorithms 37 (1) (2004) 147–158.
[33] A. Vaccaro, C. A. Cañizares, K. Bhattacharya, A Range Arithmetic-Based Optimization Model for Power Flow Analysis Under Interval Uncertainty, IEEE Transactions on Power Systems 28 (2) (2013) 1179–1186. doi:10.1109/TPWRS.2012.2214405.
[34] H. Bludszuweit, J. A. Domínguez-Navarro, A. Llombart, Statistical Analysis of Wind Power Forecast Error, IEEE Transactions on Power Systems 23 (3) (2008) 983–991.
[35] F. De Caro, A. Vaccaro, D. Villacci, Adaptive Wind Generation Modeling by Fuzzy Clustering of Experimental Data, Electronics 7 (4) (2018) 47.